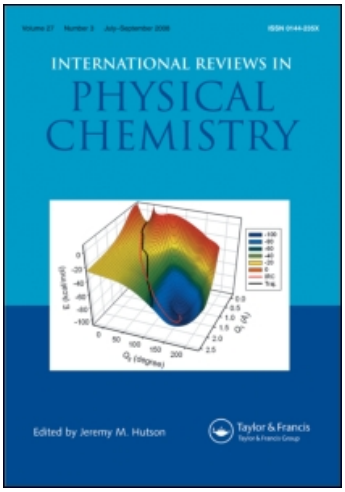

International Reviews in Physical Chemistry
Publication details, including instructions for authors and subscription information:
http://www.informaworld.com/smpp/title~content=t713724383

Importance of long-range interactions in chemical reactions at cold and ultracold temperatures

Philippe F. Weck[a]; N. Balakrishnan[a]
[a] Department of Chemistry, University of Nevada Las Vegas, Las Vegas, NV 89154, USA

To cite this Article Weck, Philippe F. and Balakrishnan, N.(2006) 'Importance of long-range interactions in chemical reactions at cold and ultracold temperatures', International Reviews in Physical Chemistry, 25: 3, 283 — 311
To link to this Article: DOI: 10.1080/01442350600791894
URL: http://dx.doi.org/10.1080/01442350600791894

International Reviews in Physical Chemistry,
Vol. 25, No. 3, July–September 2006, 283–311

Taylor & Francis
Taylor & Francis Group

Importance of long-range interactions in chemical reactions at cold and ultracold temperatures

PHILIPPE F. WECK* and N. BALAKRISHNAN

Department of Chemistry, University of Nevada Las Vegas, 4505 Maryland Parkway, Las Vegas, NV 89154, USA

(*Received 2 May 2006*)

We review the recent progress achieved in the theoretical description of chemical reactions at low temperatures. In particular, we discuss the crucial role played by the van der Waals interaction potential in quantum-mechanical scattering calculations of atom–diatom collisions in the cold and ultracold regimes, where abstraction reactions proceed by tunnelling. The importance of zero-energy resonances in enhancing the reactivity in the zero-temperature limit is assessed. The impact of Feshbach resonances associated with the decay of metastable states of van der Waals complexes on reactive scattering is addressed through a series of examples. Finally, we discuss the sensitivity of the reaction dynamics to the topology of the van der Waals well.

Contents

PAGE

1. Introduction 284

2. Atom–diatom quantum scattering at low temperatures 286
2.1. Theoretical method 286
2.2. Properties of low-temperature scattering 287

3. Reactive scattering at low energies 288

4. Sensitivity of the reaction dynamics to details of the potential energy surface 300

5. Conclusions and future prospects 305

Acknowledgments 307

References 307

*Corresponding author. Email: weckp@unlv.nevada.edu

International Reviews in Physical Chemistry
ISSN 0144–235X print/ISSN 1366–591X online
http://www.tandf.co.uk/journals
DOI: 10.1080/01442350600791894

1. Introduction

Investigations of atomic and molecular interactions at low temperatures have become a frontier area of research in recent years fuelled by the successful creation of Bose–Einstein condensates of atoms and molecules. The availability of different methods for the cooling and trapping of atoms and molecules allows the investigation of cold and ultracold collisions of a wide variety of molecular systems. The ability to cool, trap, and manipulate cold and ultracold samples of atoms and molecules has opened up a host of exciting research opportunities in physics and chemistry – quantum computing [1], tests of fundamental symmetries such as the measurement of the electric dipole moment of the electron [2], high-resolution molecular spectroscopy [3–6], experimental investigation of rovibrational energy transfer at ultralow temperatures [7–12], and coherent chemistry where reactants and products are formed in coherent quantum superpositions of states [13–17]. The achievement of Bose–Einstein condensation (BEC) of diatomic molecules [17–19] in the last few years has added considerable excitement to these studies, especially the experimental investigation of energy transfer and coherent chemistry in cold and ultracold regimes.

Current experimental efforts for cooling and trapping molecules fall into four different categories: photoassociation of ultracold atoms, Feshbach resonance method, the buffer gas cooling of paramagnetic molecules, and electrostatic cooling of polar molecules. Photoassociation spectroscopy [3, 4, 13, 14, 20] employs ultracold alkali metal atoms as precursors to create an electronically excited molecular state which decays to the ground electronic state after emitting a photon. Though the translational temperature of the molecules produced by this technique is comparable to that of the precursor atoms ($\sim\mu$K) the molecules are preferentially formed in high-lying vibrational levels of the ground electronic state and collisional quenching leading to trap loss remains a major obstacle in trapping them. The lifetime of the excited molecules is restricted by inelastic collisions leading to trap loss.

The Feshbach resonance method [17–19] which is responsible for the current success in achieving molecular BEC starts with Fermi gas of atoms that have been evaporatively cooled to a high degree of quantum degeneracy. Molecules are created by adiabatically sweeping an external magnetic field through a Feshbach resonance corresponding to the bound pair. The resulting molecules are highly vibrationally excited as in photoassociation spectroscopy. An interesting property of the molecules created from fermionic atoms is that they have relatively long lifetimes (on the order of tens or hundreds of ms) compared to those created by photoassociation of atomic BECs. The long lifetimes of BECs created from fermionic atoms have been attributed to the Pauli suppression of the quenching process. Thus, molecules created by the Feshbach resonance method may allow the possibility of studying vibrational relaxation and chemical reactivity at ultracold temperatures, a topic that has been central to the investigation of ultracold collisions over the last several years. Indeed, Chin *et al.* [12] have recently reported experimental investigations of collisions between two ultracold magnetically tuned Cs_2 dimers. The ultracold dimers were created from the corresponding atomic condensate using the Feshbach resonance technique and

inelastic two-body rate coefficients of the order of 10^{-11}–10^{-10} cm^3/s have been reported based on time-evolution of the number of molecules in the trap.

The other two techniques use either a magnetic trapping scheme [7, 9, 21, 22] that is applicable to paramagnetic molecules or an electrostatic method [23–30] that is suitable for polar molecules. The magnetic trapping scheme developed by Doyle and coworkers employs cold ^{3}He buffer gas to cool paramagnetic molecules and has been successfully applied [9] to the cooling and trapping of CaH molecules at a temperature of about 400 mK. The electrostatic method developed by Meijer and coworkers has succeeded in cooling CO molecules to 4 mK [24, 25] and deuterated ammonia molecules to about 10 mK [26, 27, 29]. Similar experiments on NH molecules are in progress. Gupta and Herschbach [31] demonstrated yet another technique which employs supersonic expansion in a rapidly rotating molecular beam resulting in molecules with sub-Kelvin translational temperatures.

Cold molecules are also finding applications well beyond the traditional boundaries. For example, Meijer and coworkers [32] recently reported direct measurement of the radiative lifetime of vibrationally excited OH radicals ($v = 1$, $J = 3/2$) decelerated using the electrostatic technique and loaded into a quadrupole trap. Infrared emission from vibrationally excited OH radicals leads to the well known Meinel system [33] and quantitative analysis of the emission relies on detailed knowledge of the Einstein A coefficient. Meijer and coworkers [32] reported a value of 59.0 ± 2.0 ms for the lifetime, in close agreement with the calculated value of 58.0 ± 1.0 ms [32]. This is an improvement over the most updated value of 56.6 ms available in the HITRAN 2004 database [34] which has an experimental uncertainty of 10–20%.

From a dynamics perspective, one of the unique aspects of ultracold collisions is the large de Broglie wavelength that makes quantum effects such as tunnelling especially important. Furthermore, recent calculations of chemical reactivity [15, 35–42] and rovibrational relaxation [43–63] in atom–molecule collisions at cold and ultracold temperatures have shown that the long-range part of the interaction potential plays an important role in the dynamics. It has been known for some time [64–68] that quasibound states of the van der Waals potential may undergo prereaction and that regions of the potential energy surface (PES) that are not in the vicinity of the transition state may influence the outcome of the reaction. The term 'prereaction' refers to the process in which a rotationally or vibrationally excited van der Waals complex decays through chemical reaction rather than rotational or vibrational predissociation. Skouteris *et al.* [66] have shown that it was necessary to employ potential surfaces that include the van der Waals part to reproduce measured values of DCl/HCl branching ratios in Cl + HD reaction. Calculations with potential energy surfaces that do not include the van der Waals interaction were unable to account for the observed branching ratio. In a recent study of the Cl + HD($v = 1$) reaction Balakrishnan [37] showed that decay of quasibound states of the Cl$\cdots$HD($v = 1$) van der Waals complexes leads to Feshbach resonances in the energy dependence of both non-reactive and reactive cross-sections and that the reactive channel leading to the HCl + D channel dominates at low energies.

The aim of this article is to provide an overview of recent studies of chemical reactivity in neutral atom–molecule collisions at cold and ultracold temperatures with special emphasis on reactions dominated by tunnelling. Obviously, this is not meant

to be a comprehensive review of chemical reactions at low temperatures but a rather biased overview taking examples from our own calculations. An excellent review of the behaviour of molecules near absolute zero and external control of molecules using magnetic field has been published by Krems [69] in a recent issue of this journal. Also, Doyle *et al.* [70] provide a very nice overview of recent research in cold molecules, with special emphasis on polar molecules.

The paper is organized as follows: In the next section we give a brief description of the scattering method adopted in much of the calculations presented here and also the behaviour of elastic and inelastic scattering at low energies. In section 3, we describe in some detail recent studies of chemical reactivity at low temperatures with specific emphasis on neutral atom–molecule reaction involving an energy barrier. In section 4, we discuss recent studies that explore sensitivity of the dynamics to details of the interaction potential taking the $O(^3P) + H_2$ reaction as an illustrative example. Section 5 concludes with an overview of future research in this field.

2. Atom–diatom quantum scattering at low temperatures

2.1. *Theoretical method*

Quantum scattering calculations of atom–diatom chemical reactions have traditionally been performed using both time-independent and time-dependent quantum-mechanical approaches. While time-dependent methods are more appropriate at higher energies, time-independent methods are preferred at low energies. The calculations reported here have all been performed using the coupled-channel hyperspherical coordinate method implemented by Skouteris *et al.* [71] to solve the time-independent Schrödinger equation for the motion of three nuclei on a single Born–Oppenheimer PES. The simultaneous expansion of the wave functions of all three chemical arrangements (A + BC, B + CA and C + AB) in the Delves hyperspherical coordinates in this implementation allows calculation of detailed state-to-state quantities of importance in collisions at low temperatures. The total wave function of the collision complex consists of a superposition of asymptotic basis functions for the different reaction arrangements, which appear particularly suited to the description of abstraction reactions, featuring a potential barrier along the reaction pathway. For insertion reactions, generally barrierless, the total wave function should be expressed instead as a combination of basis functions varying with the hyperradius. As indicated above only abstraction reactions will be discussed in this review. The reader is referred to articles [72–75] for illustrative studies of insertion reactions and recent studies of Bodo *et al.* [76, 77] for reactions involving ion-exchange.

Solution of the Schrödinger equation yields parity-adapted S-matrix elements, $S^{J,P}_{v'j'k',\,vjk}$, for all three arrangements of the collision system, where J is the total angular momentum quantum number and P is the triatomic parity eigenvalue. The quantities v and j denote the diatomic vibrational and rotational quantum numbers and k is the helicity quantum number (i.e. the angular momentum projection onto the intermolecular axis) for the reactants, their primed counterparts referring to the products.

Parity-adapted S-matrix elements are then transformed into their standard helicity representation, $S^J_{v'j'k',\,vjk}$, using the formulas [71]

$$S^J_{v'j'k',\,vjk} = S^J_{v'j'-k',\,vj-k} = \frac{\sqrt{(1+\delta_{k'0})(1+\delta_{k0})}}{2}\left[S^{J,+1}_{v'j'k',\,vjk} + S^{J,-1}_{v'j'k',\,vjk}\right] \tag{1}$$

and

$$S^J_{v'j'-k',\,vjk} = S^J_{v'j'k',\,vj-k} = (-1)^J \frac{\sqrt{(1+\delta_{k'0})(1+\delta_{k0})}}{2}\left[S^{J,+1}_{v'j'k',\,vjk} - S^{J,-1}_{v'j'k',\,vjk}\right], \tag{2}$$

where δ_{ij} is the Kronecker symbol and the helicity quantum numbers k and k' are limited to the ranges $0 \le k \le \min(J,j)$ and $0 \le k' \le \min(J,j')$. Initial state-selected probabilities can be computed as a function of the incident kinetic energy using the expression

$$P^J_{vj}(E_{\mathrm{kin}}) = \sum_{v'j'k'k} \left|S^J_{v'j'k',\,vjk}(E_{\mathrm{kin}})\right|^2, \tag{3}$$

where the summation runs over both positive and negative values of k and k'. In turn, initial state-selected energy-dependent cross-sections (excitation functions) are given by

$$\sigma_{vj}(E_{\mathrm{kin}}) = \frac{\pi}{k^2_{vj}(2j+1)} \sum_{J=0}^{J_{\max}} (2J+1) P^J_{vj}(E_{\mathrm{kin}}), \tag{4}$$

where k_{vj} is the incident channel wave vector. At low temperatures, only collisions with zero total angular momentum significantly contribute to scattering and most of the results presented here correspond to s-wave scattering in the incident channel.

2.2. *Properties of low-temperature scattering*

In the limit of vanishing kinetic energy, it is convenient to express the scattering cross-section in terms of the scattering length,

$$a_{vj} = -\lim_{k_{vj}\to 0} \frac{\delta(k_{vj})}{k_{vj}}, \tag{5}$$

where δ is the phase shift in the limit $k_{vj} \to 0$. The scattering length is real for single channel scattering where purely elastic scattering occurs but it has an imaginary part when inelastic or reactive channels are present. The complex scattering length is defined as

$$a_{vj} = \alpha_{vj} - i\beta_{vj}. \tag{6}$$

The real and imaginary parts are related to the elastic component of the S-matrix, S_{vj}^{el}, according to

$$\alpha_{vj} = -\lim_{k_{vj}\to 0} \frac{\mathrm{Im}(S_{vj}^{\mathrm{el}})}{2k_{vj}} \tag{7}$$

and

$$\beta_{vj} = \lim_{k_{vj}\to 0} \frac{1 - \mathrm{Re}(S_{vj}^{\mathrm{el}})}{2k_{vj}}. \tag{8}$$

A large and positive value of the real part of the scattering length is an indicator of the presence of a near-zero energy bound/quasibound state while a large and negative value of α indicates the presence of a virtual state. The poles of the S-matrix $S(k_{vj})$ can appear on either one of the two sheets of the Riemann surface corresponding to the positive or negative axis of the complex k-plane. Virtual states correspond to poles located on the negative energy axis of the non-physical energy sheet or the complex k-plane with $\mathrm{Im}(k_{vj}) < 0$ while bound states are associated with poles located on the negative energy axis of the physical energy sheet or the complex k-plane with $\mathrm{Im}(k_{vj}) > 0$. A virtual state will become a bound state as the strength of potential is increased, during which the scattering length goes through infinity.

The elastic cross-section becomes finite in the zero energy limit and for distinguishable particles its magnitude is given by

$$\sigma_{vj\to vj}(E_{vj} \to 0) = 4\pi(\alpha_{vj}^2 + \beta_{vj}^2). \tag{9}$$

Furthermore, in the limit of zero temperature, Wigner's law [78] holds and the inelastic (reactive and non-reactive) cross-sections vary inversely with the velocity. The imaginary part of the scattering length is related to the total inelastic cross-section $\sigma_{vj}^{\mathrm{in}}$ in the limit of zero velocity [44, 79, 80]:

$$\beta_{vj} = \lim_{k_{vj}\to 0} \frac{k_{vj}\sigma_{vj}^{\mathrm{in}}}{4\pi} \tag{10}$$

where $\sigma_{vj}^{\mathrm{in}} \sim 1/k_{vj}$. Thus, the rate coefficients for inelastic processes become finite in the limit of zero temperature [44, 79, 80]

$$R_{vj}(T \to 0) = 4\pi\beta_{vj}\hbar/\mu. \tag{11}$$

3. Reactive scattering at low energies

It has long been known that rate coefficients of exothermic chemical reactions are finite at zero temperature [78] but may be very small because of reaction barriers [81–84].

However, calculations of the benchmark $F + H_2(v = 0, j = 0) \rightarrow HF(v') + H$ reaction by Balakrishnan and Dalgarno [15] showed a surprisingly large value for the rate coefficient in the limit of zero temperature despite having an energy barrier of about 400 K in the entrance channel of the reaction. The reaction is dominated by tunnelling at low temperatures and the zero temperature limiting value of the rate coefficient is found to be about $1.25 \times 10^{-12}\,cm^3\,s^{-1}$ using the FH_2 potential energy surface developed by Stark and Werner (SW) [85]. While there is a considerable body of published work on the dynamics of $F + H_2/HD/D_2$ reactions [65, 67, 86–107], here we focus mainly on the behaviour of the reaction at low and ultralow energies. Cross-sections for the $F + H_2$ reaction for total angular momentum quantum number $J = 0$ resolved into individual vibrational levels of the product HF molecule summed over all final rotational levels are depicted in figure 1. It is seen that in the limit of vanishing collision energies, below 10^{-5} eV, cross-sections vary inversely as the collision velocity in accordance with Wigner's threshold law [78]. The energy dependence of the cross-sections is characterized by the presence of oscillatory structures near 10^{-2} eV which originate from resonant states associated with quasibound levels supported by the van der Waals well in the product channel [89, 90]. Figure 1 shows preferential formation of vibrationally excited $HF(v')$ molecules, including in the zero-temperature limit, consistent with the behaviour observed at high temperatures.

The unusually large value of the limiting rate coefficient for the $F + H_2$ reaction motivated further studies of it and its isotopic counterparts [35, 108–111]. Balakrishnan and Dalgarno [35] investigated the $F + HD(v = 0, j = 0)$ reaction at ultralow energies and showed that the rate coefficient for HF formation is about a factor of 5.5 larger than that of DF formation in the limit of zero-temperature, consistent with the findings of Baer and coworkers [93, 98] and Kornweitz and Persky [106]

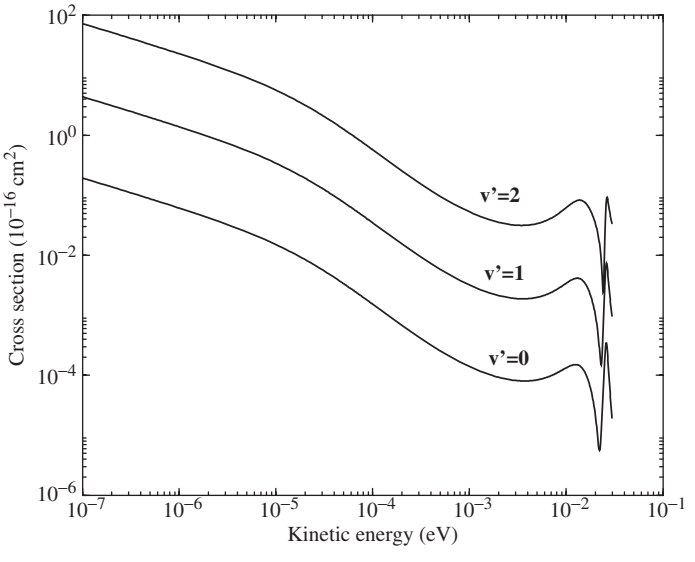

Figure 1. Product vibrational state resolved cross-sections for the $F + H_2(v = 0, j = 0) \rightarrow HF(v') + H$ reaction as a function of the incident kinetic energy.

at higher temperatures. The higher probability for HF formation at low energies is attributed to the more efficient tunnelling of the lighter H atom compared to the heavier D atom. Chemical reaction leading to HF formation was also found to dominate in *s*-wave scattering in $F + HD(v = 0, j = 1)$ reaction for $J = 1$ compared to pure rotational quenching. This is in contrast to the $F + D_2$ reaction for which Bodo *et al.* [108] found that in the limit of zero temperature non-reactive rotational quenching dominates in collisions of F atoms with rotationally excited D_2 molecules. Bodo and Gianturco [110] also investigated the effect of vibrational excitation in $F + H_2$ and $F + D_2$ reactions and found that the reactivity increases significantly with one quantum vibrational excitation of the H_2 and D_2 molecules. They found that chemical reaction dominates over vibrational quenching in $F + H_2(v = 1)$ and $F + D_2(v = 1)$ reactions.

In order to further investigate the behaviour of $F + H_2$ and $F + D_2$ reactions at ultracold temperatures, Bodo *et al.* [111] performed detailed analysis of the behaviour of elastic and inelastic scattering of these systems at energies close to the rection threshold. Cumulative reaction probabilities and cross-sections for the $F + H_2 (v = 0, j = 0) \rightarrow HF + H$ and $F + D_2(v = 0, j = 0) \rightarrow DF + D$ reactions on the SW PES [85] obtained by Bodo *et al.* [111] are presented in figure 2. It is seen that the reaction probabilities for H_2 and D_2 exhibit very different energy dependences. In the zero-energy limit, reaction cross-sections for H_2 are up to 2 orders of magnitude larger than for D_2. The large difference in reactivity for the H_2 and D_2 reactions cannot be explained on the basis of mass difference alone. It has been shown that part of the difference can be attributed to the presence of a virtual state lying close to the threshold of the entrance channel of the $F + H_2$ reaction. In particular, this virtual state is responsible for the maximum in the reaction probability and the corresponding curvature in the reaction cross-section at 3×10^{-5} eV of collision energy. Evidence for the virtual state is further supported by the detection of a deep Ramsauer–Townsend minimum in the elastic component of the total cross-section for $F + H_2$ scattering at collision energies in the vicinity of 3×10^{-5} eV [111] and a negative value for the real part of the scattering length.

Since the behaviour of the $F + H_2$ and $F + D_2$ reaction probabilities are dramatically different in the limit of zero kinetic energy, Bodo *et al.* [111] showed that the reaction dynamics could be explored by performing calculations of scattering matrix in which the mass of the H or D atoms is replaced with a fictitious mass ranging from 0.5 to 2.0 hydrogen atom masses. Results of these calculations are reproduced in figure 3 for the real part of the scattering length (upper panel), zero-temperature limiting rate coefficient (middle panel) and the binding energy of the least bound state (bottom panel). The upper panel of figure 3 shows the variation of α_{00} as a function of the mass of the pseudo-atom. A discontinuous changeover from $+\infty$ to $-\infty$ appears at 1.12 hydrogen masses as a signature of the resonant passage of the uppermost quasi-bound state to a virtual state in the continuum. Correspondingly the zero-temperature reaction rate coefficient exhibits a maximum value of $10^{-9}\,cm^3 s^{-1}$. The lower panel of figure 3 shows that the energy of the uppermost quasibound state decreases gradually with the mass of the pseudo-hydrogen atom as the continuum is approached and rapidly varies when this resonant state enters the continuum to finally weaken as the newly formed virtual state propagates to higher energies.

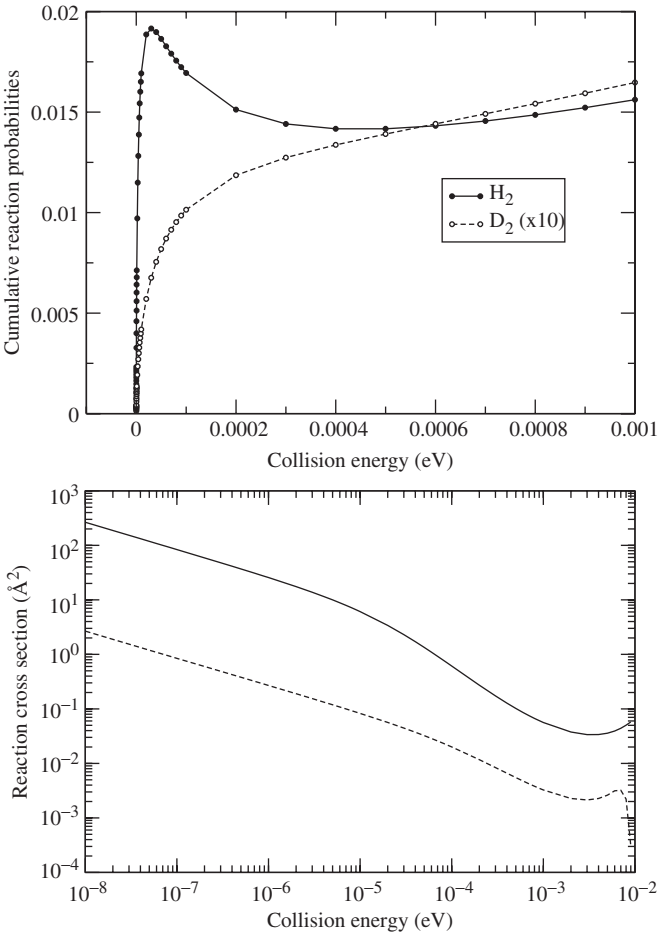

Figure 2. Cumulative probabilities (upper panel) and cross-sections (lower panel) for the $F + H_2 \rightarrow HF + H$ (solid curve) and $F + D_2 \rightarrow DF + D$ reactions (dashed curve).

It is interesting to point out that the behaviour of the scattering length with reduced mass of the collision system shown in figure 3 is in striking similarity to the variation of scattering length with external magnetic field in the vicinity of a Feshbach resonance [18–20]. In the Feshbach resonance technique, the energy of two free atoms is matched to that of a quasibound molecular state by varying the strength of an applied magnetic field. This allows control of the *s*-wave scattering length and hence the interaction strength from repulsive ($a > 0$) to attractive ($a < 0$).

As indicated in section 2.2, when zero-energy resonances are present the elastic scattering cross-section attains large values in the limit of zero kinetic energy. This is illustrated in figure 4 for elastic scattering in $Ar + D_2(v = 1, j = 0)$ collisions from recent calculations of Uudus *et al.* [112]. It is seen that the zero-energy limit of the $Ar + D_2$ elastic cross-section is about two orders of magnitude larger than for

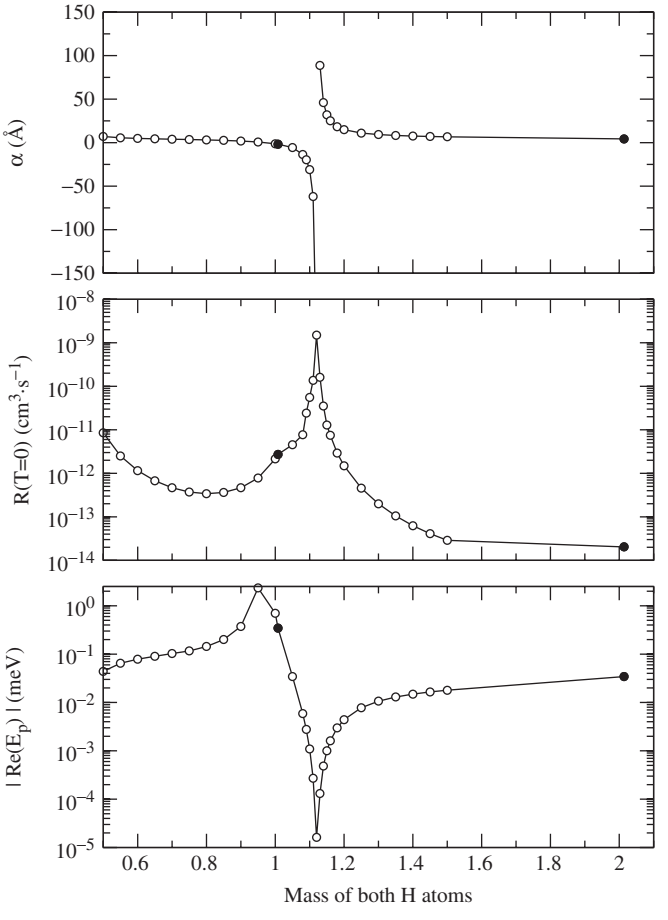

Figure 3. Real part of the scattering length (upper panel), zero-temperature values of the rate constant (middle panel) and positions of quasibound and virtual states (lower panel) of the F···H_2 complex as functions of the mass of a pseudo-hydrogen atom.

the case of $Ar + H_2(v = 1, j = 0)$ collisions. The large value of the elastic scattering cross-section for the Ar + D_2 system is due to the presence of a quasibound state close to the continuum of the adiabatic potential correlating with the $v = 1, j = 0$ channel of the D_2 molecule. However, no such quasibound state exists for the Ar + H_2 system. The calculations for both systems are performed using the potential energy surface of Bissonnette *et al.* [113]. To explore the sensitivity of the dynamics to details of the interaction potential, Uudus *et al.* [112] performed scattering calculations of the $Ar + H_2(v = 1, j = 0)$ system using the potential surface of Schwenke *et al.* [114] which yielded results almost indistinguishable from those obtained using the potential surface of Bissonnette *et al.* [113] as illustrated in figure 4. The binding energy of the quasibound state responsible for the zero-energy resonance in Ar + D_2 collisions was found to be $6.0 \times 10^{-4}\text{cm}^{-1}$ [112]. The scattering length approximation can also be

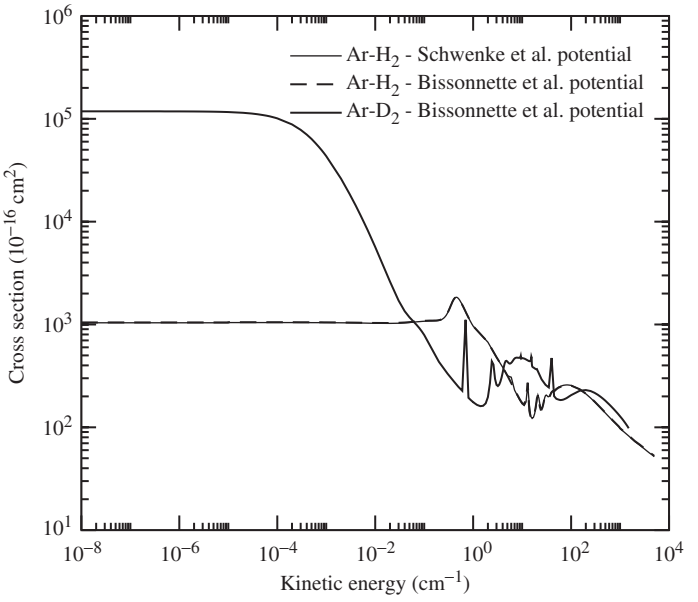

Figure 4. Energy dependence of the elastic cross-sections for $Ar + H_2(v = 1, j = 0)$ and $Ar + D_2(v = 1, j = 0)$ collisions.

used to evaluate binding energy of the least bound state (quasibound state closest to the channel threshold):

$$|E_b| = \frac{\hbar^2}{2\mu\alpha_{10}^2}, \tag{12}$$

where μ is the reduced mass of the $Ar - D_2$ system and α_{10} is the real part of the scattering length for the $v=1$, $j=0$ level. This yields a binding energy $|E_b| = 4.9 \times 10^{-4}\text{cm}^{-1}$. A more accurate value of the binding energy is obtained using the effective range theory [46]:

$$|E_b| = \frac{\hbar^2}{\mu r_{vj}^2}\left(1 - \frac{\alpha_{vj} r_{vj}}{|a_{vj}|^2} - \sqrt{1 - \frac{2\alpha_{vj} r_{vj}}{|a_{vj}|^2}}\right), \tag{13}$$

where r_{vj} is the effective range of the potential. The effective range formula yields a value of $|E_b| = 5.95 \times 10^{-4}\,\text{cm}^{-1}$ in close agreement with the observed value of $6.0 \times 10^{-4}\,\text{cm}^{-1}$. The effective range theory can also be used to evaluate the width of the resonances [46]:

$$\Gamma_{vj} = \frac{2\hbar^2 \beta_{vj}}{\mu r_{vj} |a_{vj}|^2}\left(\left[1 - \frac{2\alpha_{vj} r_{vj}}{|a_{vj}|^2}\right]^{-1/2} - 1\right), \tag{14}$$

which yields $\Gamma_{10} = 1.03 \times 10^{-14}\,\text{cm}^{-1}$ for the resonance in $Ar + D_2$ system.

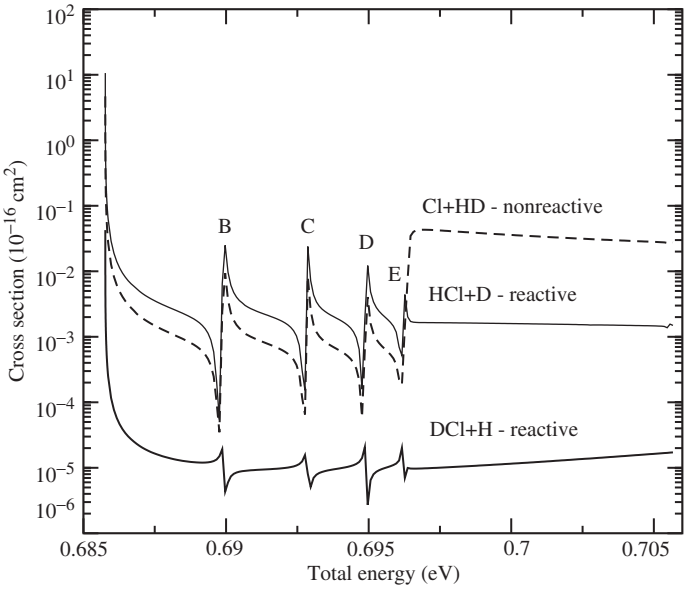

Figure 5. Reactive and non-reactive cross-sections for $Cl + HD(v = 1, j = 0)$ collisions as a function of the total energy. Resonances corresponding to quasibound levels represented in figure 6 are indicated by letters.

In addition to zero-energy resonances, Feshbach resonances arising from the decay of metastable states supported by van der Waals wells in the initial or final channels may also strongly influence the energy dependence of reactive and non-reactive cross-sections at low energies [37, 68, 89]. Here, we illustrate how decay of quasibound states of the $Cl\cdots HD(v=1)$ complex formed in Cl + HD($v=1$) collisions influences reactivity at low energies. The Cl + H_2/HD/D_2 reactions have been the topics of considerable theoretical and experimental attention [101, 115–127] but all these studies focused on the dynamics at higher temperatures. Here, we explore the dynamics at cold and ultracold temperatures where the van der Waals part of the interaction potential plays a decisive role in the dynamics. Cross-sections for HCl and DCl formation and non-reactive rovibrational transitions in $Cl + HD(v = 1, j = 0)$ collisions for $J=0$ calculated by Balakrishnan [37] using the potential energy surface of Bian and Werner [119] are displayed in figure 5 as functions of the total energy in the vicinity of the reaction threshold. These resonances labelled by the letters B, C, D, and E result from predissociation or prereaction of van der Waals complexes in the entrance channel of the collisions since they are reproduced in all three product channels. One way to proceed to identify these resonances is to construct adiabatic potentials as a function of R obtained from diagonalizing the diabatic potential energy matrix in a basis set of the rovibrational levels of the HD molecule and then calculate the eigenvalues and the corresponding wave functions [128, 129]. Figure 6 shows the adiabatic potentials correlating with $v = 1$, $j = 0$ and $v = 1$, $j = 1$ levels of the HD molecule as functions of the atom–molecule separation, R, and the quasibound states A, B, C, D, and E supported by the latter. While the metastable state denoted by A is not

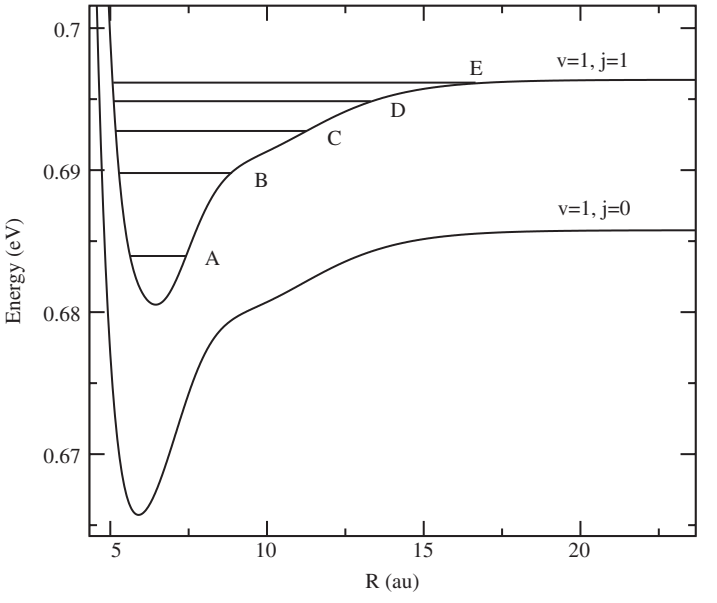

Figure 6. Adiabatic potential energy curves of the Cl + HD system correlating to the HD($v = 1$, $j = 0$) and HD($v = 1$, $j = 1$) levels as functions of the atom–molecule separation, R. Quasibound levels responsible for the resonances observed in figure 5 are labelled by B, C, D and E.

accessible from scattering in the $v = 1$, $j = 0$ channel, quasibound levels B to E undergo vibrational prereaction or predissociation and are responsible for the resonances depicted in figure 5. Wave functions of the quasibound states B and E, the deepest and the least bound ones shown in figure 6 are presented in figure 7 as functions of R. Although the wave function of the quasibound state E extends far away from the transition state region of the reaction, it preferentially undergoes prereaction leading to HCl + D product rather than predissociation to yield Cl + HD($v = 0$) product.

Figure 8 shows cross-sections calculated by Balakrishnan [37] for reactive and non-reactive scattering in Cl + HD($v = 1$, $j = 0$) collisions as functions of the incident kinetic energy ranging from the ultracold to near thermal limits. The DCl/HCl branching ratio reaches a limiting value of 4.0×10^{-3} in the Wigner regime. Prereaction of the Cl$\cdots$H − D van der Waals complexes in the initial channel leading to HCl formation is more favorable than predissociation or prereaction resulting in DCl production due to the less efficient tunnelling of the D atom when tunnelling becomes the dominant reaction mechanism. The non-reactive cross-section becomes much larger than the cross-section for HCl formation beyond $E_{\mathrm{kin}} = 10^{-2}$ eV as rotational excitation to $v = 1$, $j = 1$ level becomes energetically favorable. The above results for the Cl + HD reaction demonstrate that regions of the potential energy surfaces far away from the transition state region may have significant effect on reactivity even at low temperatures.

Currently, there is considerable interest in creating dense samples of cold and ultracold polar molecules. The buffer gas cooling method and the stark-decelerator

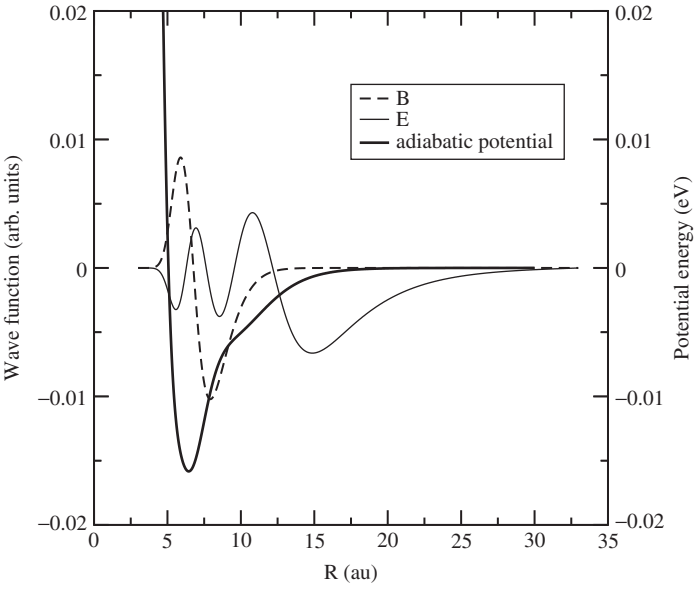

Figure 7. Wave functions of the quasibound levels B and E supported by the adiabatic potential shown in figure 6 as functions of the atom–molecule separation. Amplitudes of the wave functions have been reduced by a factor of 10 for practical plotting reasons.

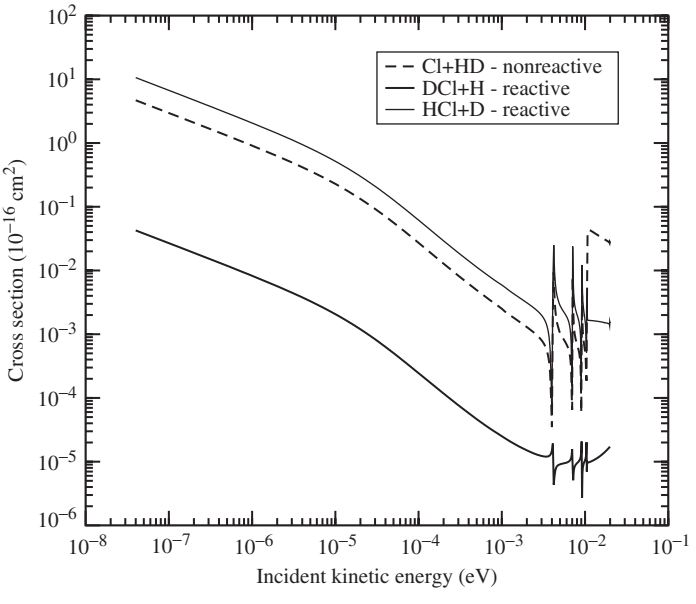

Figure 8. The same as in figure 5 but plotted as a function of the incident kinetic energy to illustrate the low-temperature behaviour of the cross-sections.

methods are especially suited for polar molecules and polar molecules are expected to play an important role in field-controlled ultracold chemistry. Since long-range interaction is generally more significant in polar molecules they provide ideal candidates for the investigation of chemical reactions at low temperature where long-range forces play an important role. In this context, we have performed extensive calculations of the Li + HF system which supports a large number of quasibound states in the entrance and exit channels due to the attractive interaction potential.

The Li + HF reaction has been the topic of numerous experimental and theoretical studies and it is a prototype system for experimental studies of the 'harpoon' mechanism in reactions between alkali or alkaline earth metal atoms and hydrogen halide molecules [130]. Thus, a large number of experimental [131–139] and theoretical studies [133–135, 138, 140–148] has been reported on the system.

The LiHF system is also a particularly interesting candidate for the study of chemical reactivity at low temperatures because both H + LiF and Li + HF reactions involve tunnelling of the relatively heavy F atom. The $LiH(X^1\Sigma^+) + F(^2P)$ product channel is highly endoergic and is not accessible at low incident kinetic energies. The strong dipole electric field of the HF molecule is responsible for an exceptionally deep van der Waals well of about 0.24 eV for the $Li \cdots F - H$ complexes, while the van der Waals well corresponding to $H \cdots F - Li$ complexes is about 0.07 eV deep. Cross-sections for LiF formation and non-reactive scattering in Li + HF ($v = 0, 1, j = 0$) collisions calculated by Weck and Balakrishnan [38] using the X^2A' LiHF ground state PES of Aguado *et al.* [149] are displayed in figure 9 as functions of the incident translational energy. Reactivity of HF($v = 0, j = 0$) molecules is small due to the inefficient tunnelling of the relatively heavy fluorine atom. In figure 9 the

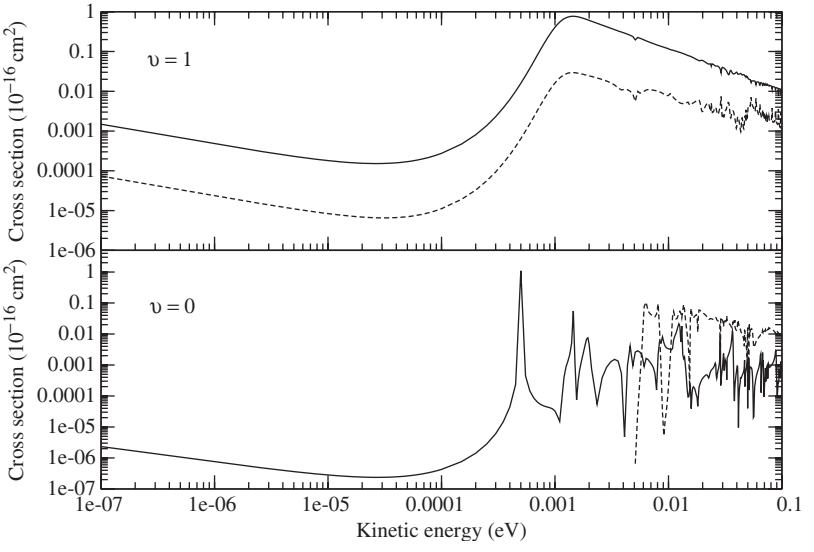

Figure 9. Cross-sections for LiF formation and non-reactive scattering in Li + HF($v, j = 0$) collisions, for $v = 0$ (lower panel) and $v = 1$ (upper panel), as a function of the incident kinetic energy. Dashed curve: non-reactive scattering; solid curve: LiF product channel.

strong peak at 5×10^{-4} eV where the probability vary by about six orders of magnitude is a reactive scattering resonance and it illustrates the importance of tunnelling in low temperature chemistry even when heavy atoms are involved. For incident kinetic energies beyond 10^{-3} eV the reaction cross-section for $v=0$ is also characterized by strong Feshbach resonances originating from quasibound states of the van der Waals complexes in the initial channel supported by adiabatic potentials correlating with $j=1-4$ of the $\mathrm{Li}\cdots\mathrm{HF}(v=0,j)$ molecule. It was found that the van der Waals complexes with high-lying stretching vibrational quantum numbers, t, generate resonances for $j=1,2$, while low-t channels give rise to resonances for $j=3,4$ [38]. Beyond 5×10^{-3}eV, non-reactive channels of the $\mathrm{Li}+\mathrm{HF}(v=0,\ j=0)$ open up and non-reactive scattering becomes more favorable than reactive scattering. This contrasts with $\mathrm{Li}+\mathrm{HF}(v=1,\ j=0)$ collisions for which the reactive channel dominates the non-reactive processes, with the LiF/HF branching ratio reaching 20 in the Wigner regime. The reaction cross-section involving excited $\mathrm{HF}(v=1,\ j=0)$ reactants are 635 times larger than with $\mathrm{HF}(v=0,\ j=0)$ reagents, thus showing that vibrational excitation significantly enhances chemical reactivity at low temperatures.

Figure 10 shows cross-sections calculated by Weck and Balakrishnan [39] for HF formation and non-reactive scattering in $\mathrm{H}+\mathrm{LiF}(v=0-2,\ j=0)$ collisions as a function of the incident translational energy. Non-reactive scattering is the dominant collision process at low temperatures. The presence of kinetic energy thresholds in the reactive and non-reactive $\mathrm{H}+\mathrm{LiF}(v=0,\ j=0)$ cross-sections stems from the fact that the reaction leading to HF formation and for rotational excitation to $\mathrm{LiF}(v=0,\ j=1)$ have endoergicities of 0.0112 eV and 3×10^{-4} eV, respectively.

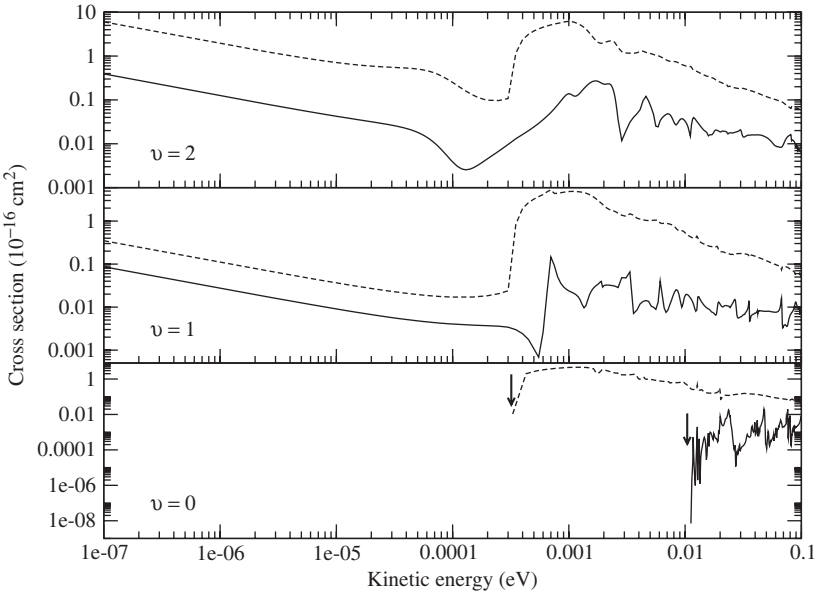

Figure 10. Cross-sections for HF formation and non-reactive scattering in $\mathrm{H}+\mathrm{LiF}(v=0-2, j=0)$ collisions as a function of the incident kinetic energy. solid curve: HF product channel; dashed curve: non-reactive scattering. For $v=0$, arrows indicate energy thresholds.

As for the Li + HF reaction, cross-sections are characterized by strong Feshbach resonances beyond 10^{-4}eV. Bound- and quasibound states calculations show that for the H + LiF($v = 0$) reaction, resonances are essentially due to the decay of ($v = 0, j, t$) metastable states of the Li $\cdots$ HF exit channel van der Waals complexes, with j and t ranging from relatively high t'-values for $j' = 1$ to the lowest-lying stretching vibrational states of $j' = 5$, while relatively few resonances originate from the H $\cdots$ LiF($v = 0$, $j = 10 - 15$, $t = 1 - 2$) states of the entrance channel complexes. Feshbach resonances tend to get washed off from the reaction cross-sections with vibrational excitation of the reactants. For $v = 1, 2$, Feshbach resonances associated with low-t states of the adiabatic potentials correlating with $j = 2 - 12$ of the entrance channel H $\cdots$ LiF complex are dominant, while only a few high-lying stretching vibrational states of the Li $\cdots$ HF($v = 1$, $j = 6$) and ($v = 2$, $j = 9$) van der Waals complexes in the exit channel give rise to resonances. Although the Li $\cdots$ HF van der Waals well is much deeper than the H $\cdots$ LiF well in the entrance channel of the reaction, it plays only a significant role in the dynamics of the H + LiF($v = 0$) reaction.

Rate coefficients calculated by Weck and Balakrishnan [39] for HF formation and inelastic scattering in H + LiF($v = 1, 2, j = 0$) collisions are presented in figure 11. As discussed in section 2, the rate coefficients for exothermic chemical reaction or inelastic scattering becomes finite in the limit of zero-temperature. Zero-temperature reaction rate coefficients for $v = 1, 2$ are significantly larger than for reactions involving tunnelling of atoms lighter than fluorine. As observed recently by Zuev *et al.* [150] for carbon tunnelling in ring expansion reactions of 1-methylcyclobutylhalocarbenes at 8 to 25 K, the results of Li + HF/H + LiF reactions suggest that heavy atom tunnelling may play a role more important than usually recognized in low-temperature chemistry.

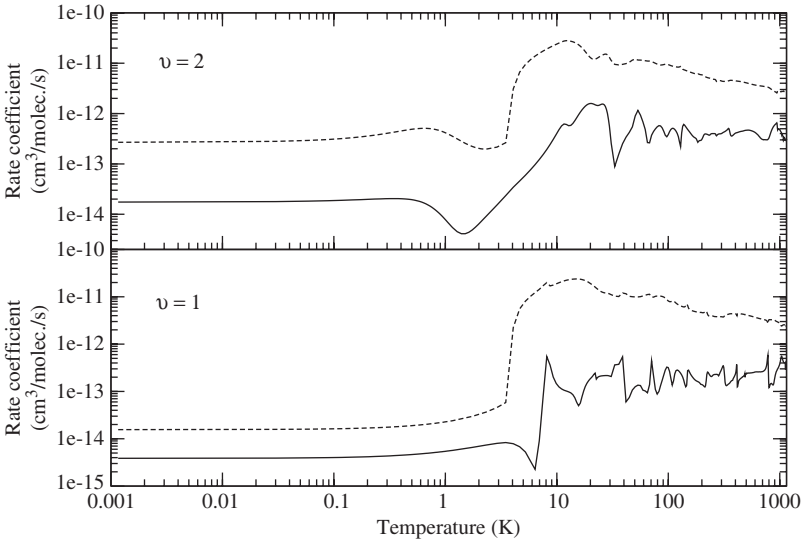

Figure 11. Temperature dependence of reaction rate coefficients for HF formation and non-reactive vibrational quenching in H + LiF($v = 1, 2, j = 0$) collisions.

4. Sensitivity of the reaction dynamics to details of the potential energy surface

One of the major challenges in the accurate description of low-energy molecular collision dynamics is the accuracy of the interaction potential. The results presented in the previous section have all been computed using potential energy surfaces developed for describing reactions occurring at thermal energies. What kind of accuracy is needed for dynamics calculations at cold and ultracold systems depends on the specific system under investigation and it is difficult to quantify in the absence of experimental data. Although figure 4 shows remarkable agreement between scattering calculations performed at low temperatures using different potential energy surfaces for the $Ar + H_2$ system, this is generally not the case. Indeed, for the same system, vibrational quenching cross-sections derived from the two potentials show significant differences at low energies [112]. Also, calculations by Soldán *et al.* [151] revealed strong sensitivity of the dynamics of three spin-polarized alkali-metal atoms systems to three-body non-additive forces. Here we focus on the sensitivity of reactive collisions to details of the long-range interaction potential by taking $O(^3P) + H_2$ reaction as an illustrative example. The $O(^3P) + H_2$ reaction has been the subject of a large number of dynamics calculations [152–168]† and measurements of its thermal rate coefficient [169–174] have been carried out over a wide range of temperatures. The reaction has a classical energy barrier of about 0.56 eV and at low temperatures it occurs mainly through tunnelling [172, 173]. The first crossed molecular beam experiments of the reaction was performed by Garton *et al.* [164] in 2003 and measured values of the reaction cross-sections were accurately reproduced by both time-dependent and time-independent quantum calculations [164, 168].

Quantum reactive scattering calculations by Weck *et al.* [40–42] of the $O(^3P) + H_2$ reaction provided detailed analysis of the importance of van der Waals forces in the dynamics of abstraction reactions. In these calculations, the reaction was investigated using the lowest $^3A''$ potential energy surface developed by Rogers *et al.* [162], referred to as GLDP PES, and the BMS1 and BMS2 surfaces developed by Brandão *et al.* [176] based on the *ab initio* data calculated by Rogers *et al.* in the vicinity of the abstraction saddle-point. Differences between these potential energy surfaces result essentially from the different fitting methods used to produce these surfaces as well as the description of the van der Waals well associated with the O···H–H complexes. The generalized London–Eyring–Polanyi–Sato double-polynomial (GLDP) method, with addition of virtual points to remove unphysical features, was used in [162] to fit the surface built from *ab initio* data, while the BMS1 and BMS2 surfaces were fitted using the double many-body expansion (DMBE) formalism. In addition, Brandão *et al.* used a semiempirical functional form to explicitly account for the R^{-n} radial dependence characteristic of long-range interactions, while the GLDP surface of Rogers *et al.* [162] provides only a partial description of these interactions. This modification deepens the van der Waals well at collinear abstraction geometry ($C_{\infty v}$ symmetry), compared

†The rate coefficients given in table 1 and by the solid and dashed curves in figure 6 of [165] should be multiplied by two. The factor of two arises from the symmetry factor in the rotational partition function of the H_2 molecule that was not included in the calculations.

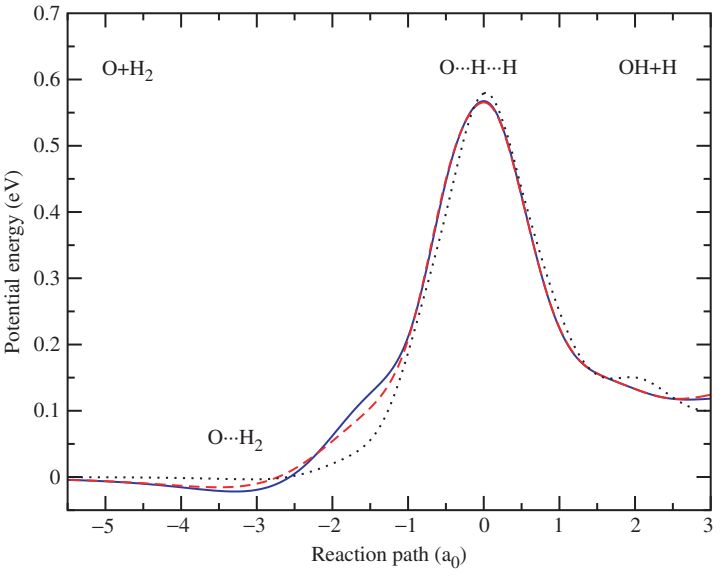

Figure 12. [Colour online] Energy profile along the minimum energy reaction pathway for $O + H_2$. Solid curve, BMS1 PES [176]; dashed curve, BMS2 PES [176]; dotted curve, GLDP PES [162].

to the GLDP PES for which the $^3\Sigma$ PES ($^3A''$ at C_s geometries) has been neglected. The BMS1 surface, resulting from the best fitting, features a van der Waals well with energy minima of 22meV and 12meV, respectively, for the $C_{\infty v}$ and C_{2v} geometries of the $O \cdots H - H$ complex. The BMS2 PES, obtained by recalibration of the BMS1 surface to reduce the depth of the van der Waals potential, is characterized by van der Waals well depths of 15meV and 9meV for $C_{\infty v}$ and C_{2v} configurations, respectively, the former being close to the value of 9meV along the minimum-energy path of the GLDP PES. The minimum energy paths for the title reaction on the three PESs are depicted in figure 12.

Probabilities calculated by Weck and Balakrishnan [40] for OH formation in $O + H_2(v = 1 - 3,\ j = 0,\ J = 0)$ collisions on the GLDP, BMS1, and BMS2 PESs are reproduced in figure 13. Probabilities computed using the BMS1 PES, which accurately describes long-range interactions, should be regarded as more reliable than those obtained with the BMS2 PES featuring a shallower van der Waals well. Calculations performed on the GLDP PES should be considered only as qualitative since the long-range interaction is only marginally accounted for. In the Wigner regime, reaction probabilities for $v = 2, 3$ computed using the BMS1 and BMS2 PESs are several orders of magnitude larger than the probabilities obtained using the GLDP PES due to the different descriptions of the van der Waals wells. Differences between the limiting values of the reactivity for the BMS1 and BMS2 PESs arise from zero-energy resonance enhancement. Using the scattering length approximation, the binding energies of the quasibound states responsible for these resonances on the BMS1 PES for $v = 1$ and on the BMS2 PES for $v = 3$ were calculated to be, respectively, $E_b = 5.55 \times 10^{-7}$eV and $E_b = 8.42 \times 10^{-7}$eV, while a virtual state at

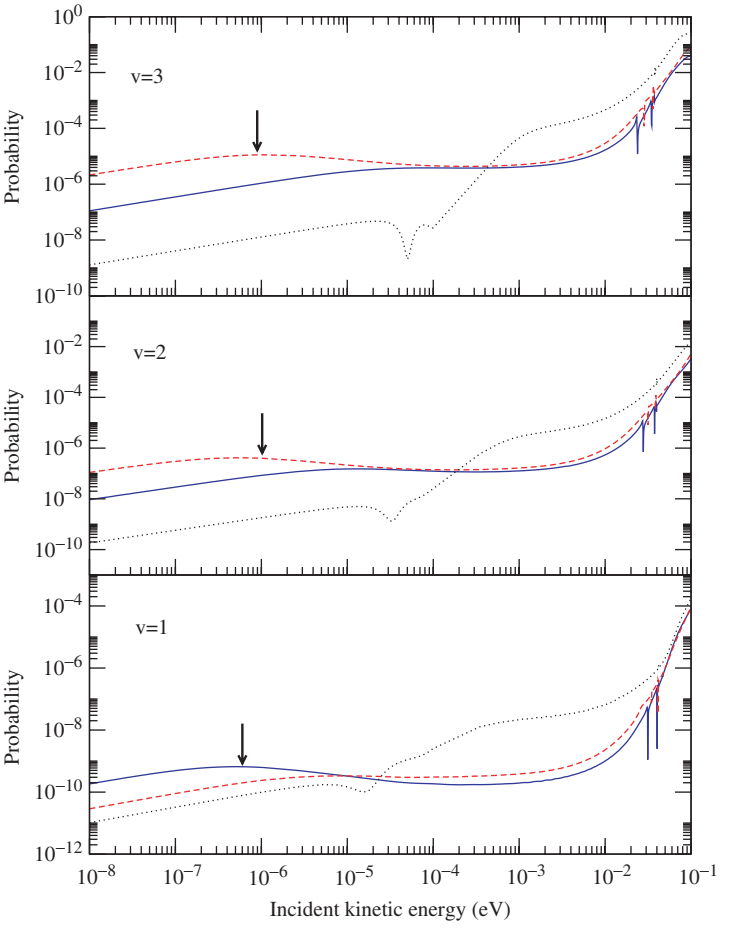

Figure 13. [Colour online] Probability for OH formation in $O + H_2(v = 1-3, j = 0, J = 0)$ collisions as a function of the incident kinetic energy. The arrows indicate the positions of quasibound levels responsible for zero-energy resonances on the different PESs. Same conventions as in figure 12 for the PESs.

$E = 1.12 \times 10^{-6}$ eV in the continuum was found responsible for the reactivity enhancement on the BMS2 PES for $v = 2$. Beyond the translationally cold energy regime, reactivity enhancement due to zero-energy resonances tends to disappear and reaction probabilities become higher for potentials with shallower van der Waals wells. The decrease of the GLDP/BMS1 probability ratio with vibrational excitation in this energy range also suggests that the influence of the van der Waals interaction fades out. For translational energies in the range 0.02–0.06 eV, Feshbach resonances appear in the $v = 1-3$ reaction probabilities. Weck and Balakrishnan [40] have shown that these resonances arise from the decay of metastable states of the $O\cdots H_2$ van der Waals potential in the entrance channel correlating with the $H_2(v = 1-3, j = 2)$ manifolds. As illustrated in figure 14, the shallow van der Waals well of the GLDP PES supports only one quasibound state, while the deeper BMS2

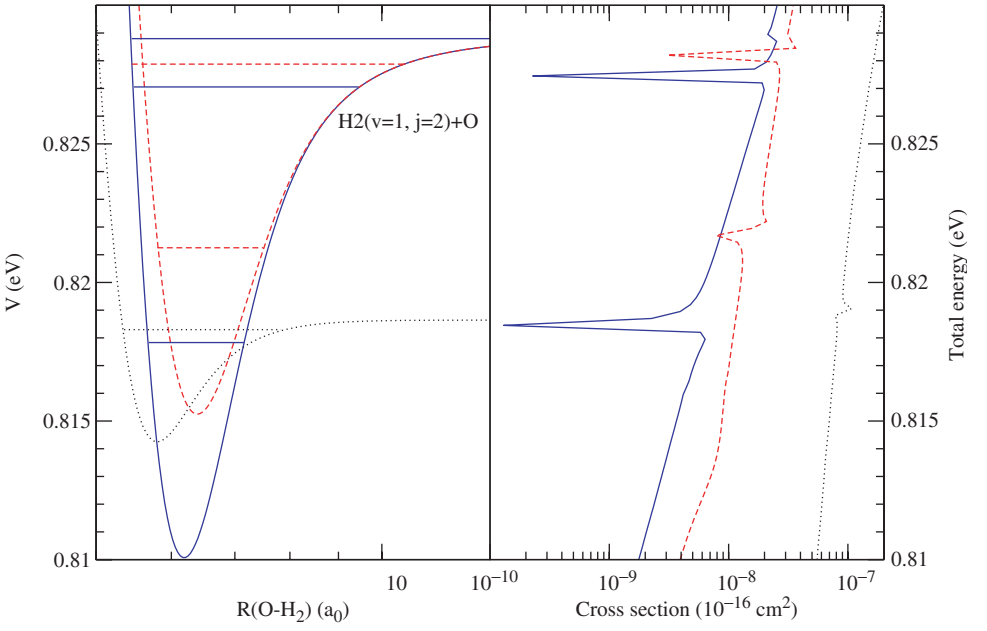

Figure 14. [Colour online] Adiabatic potential energy curves and corresponding quasibound levels of the $O\cdots H_2(v=1,\ j=2)$ van der Waals complexes (left panel); cross-section for OH formation in $O+H_2(v=1,\ j=0,\ J=0)$ collisions as a function of the total energy (right panel). Resonances in the cross-sections appear as a result of the decay of quasibound states of the $O\cdots H_2$ van der Waals complex. Same conventions as in figure 12 for the different PESs.

and BMS1 van der Waals wells allow two and three metastable states, respectively. In addition, the positions of the resonances in the energy dependence of the reaction cross-sections appear shifted for the different PESs as a result of the different geometries of the van der Waals wells. Quasiclassical trajectory (QCT) reaction probabilities in $O+H_2(v=1-3,\ j=0)$ as a function of the collision energy reported by Weck *et al.* [41] are displayed in figure 15, superimposed on quantum reactive results from figure 14. Although fair agreement is observed between quantal and classical probabilities, no reactivity is predicted by the QCT method at low translational energies reflecting the fact that QCT calculations neglect tunnelling, the preponderant reaction mechanism at low temperatures. Vibrational excitation of the reagents shifts the QCT reaction thresholds to lower energies since less incident kinetic energy is needed to overcome the reaction barrier.

Figure 16 shows integral reaction cross-sections in $O+H_2(v=1,\ j=0)$ collisions computed by Weck and Balakrishnan [42] on the GLDP, BMS1, and BMS2 PESs. Integral reaction cross-sections associated with the BMS1 and BMS2 PESs and including contributions for $0\leq J\leq 10$ appear largely dominated in the cold and ultracold regimes by $J=0$ probabilities represented in figure 13. However, the energy dependence of the integral cross-section calculated on the GLDP surface is marked by a strong resonance near $\approx 3\times 10^{-5}$ eV of incident kinetic energy. Partial reaction

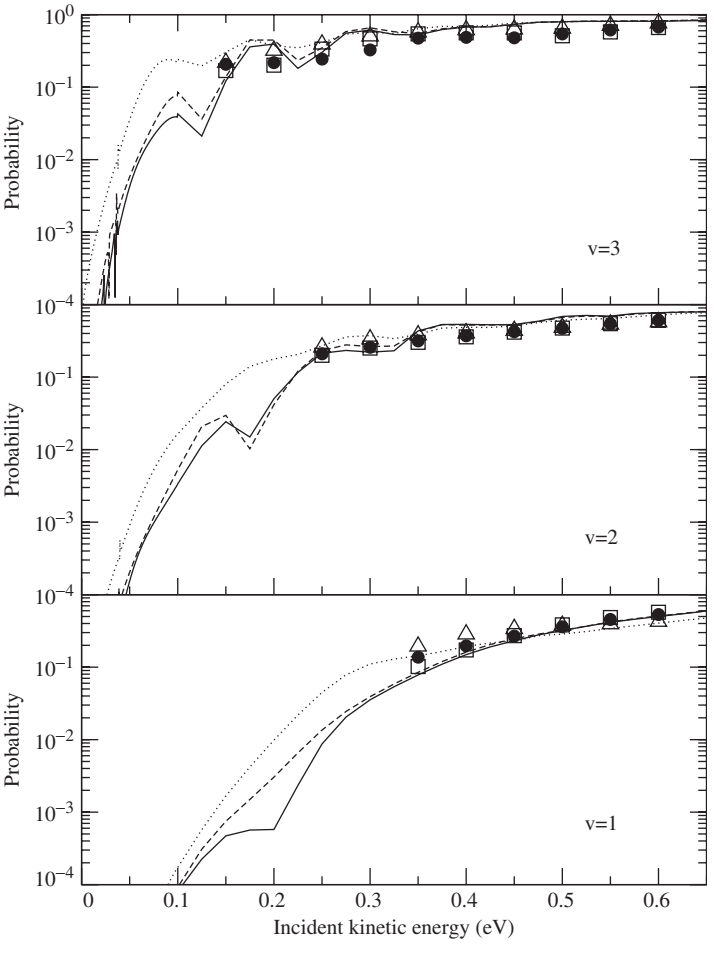

Figure 15. Quasiclassical trajectory and quantum mechanical probabilities for OH formation in $O + H_2(v = 1 - 3, j = 0)$ collisions. QCT results are represented by symbols: Filled circle, BMS1 PES [176]; square, BMS2 PES [176]; triangle, GLDP PES [162]. Same conventions as in figure 12 for the quantum mechanical results (curves).

cross-sections represented in figure 17 suggest that a shape resonance associated with the $J = 2$ component ($l = 2$ partial wave) is responsible for this increase of reactivity in the energy dependence of the integral cross-section calculated on the GLDP surface.

While the results shown here are exploratory calculations, which could be termed 'numerical experiments' on the behaviour of chemical reactions at ultracold temperatures, further progress needs to be made in cooling, trapping and manipulating cold and ultracold molecules before chemical reactivity in ultracold gases could be investigated experimentally and theoretical predictions verified. Most systems described here have been well studied at high temperatures and the results highlighted here provide illustrative aspects of chemical reactivity at low temperatures.

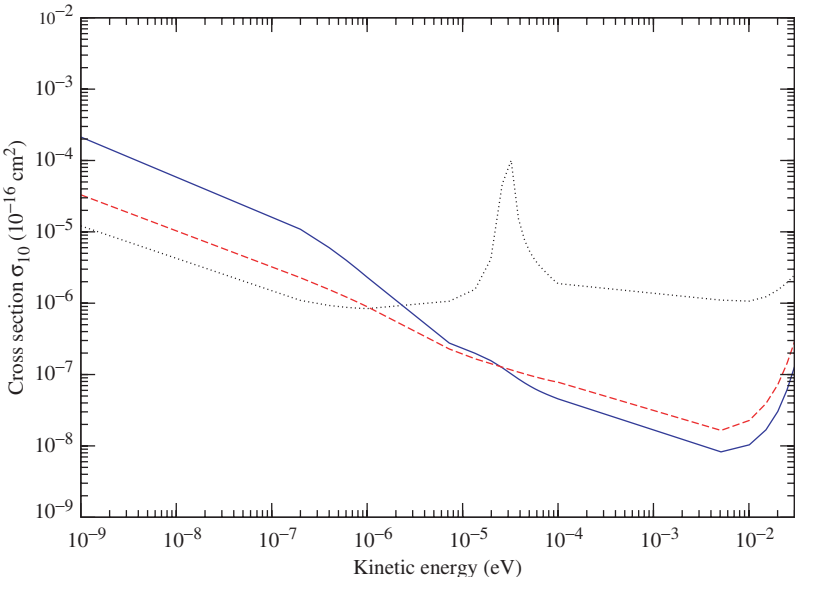

Figure 16. [Colour online] Integral cross-sections for $O + H_2(v = 1, j = 0) \rightarrow OH + H$ collisions as a function of the incident kinetic energy. Total angular momentum partial waves $0 \leq J \leq 10$ have been included in the calculations. Same conventions as in figure 12 for the different PESs.

5. Conclusions and future prospects

The investigation of cold and ultracold collisions for a wide variety of molecular systems shows the importance of quantum-mechanical effects in collision dynamics at low temperatures. Although reactivity is usually small for abstraction reactions at low collision energies since tunnelling through a potential barrier is the dominant reaction pathway, zero-energy resonances are found to enhance reactivity by several orders of magnitude in the zero-temperature limit. Feshbach resonances associated with the decay of metastable states of van der Waals wells in the entrance or exit channel of the reaction also significantly affect the reactivity. The positions and characteristics of these resonances show a strong sensitivity to the topology of the long-range part of the interaction potential, thus they can be used as powerful diagnostic tools to probe the finer details of potential energy surfaces in the tunnelling regime. Studies of quantum reactive scattering properties at low temperatures using different potential energy surfaces also shed light on the extend of alteration of product branching ratios by modifying the atom–molecule interaction in the tunnelling regime. On the one hand, such scattering information can assess the critical accuracy requirements in modern *ab initio* calculations in order to accurately predict chemical reactivity and energy transfer at ultralow temperatures. On the other hand, these studies are of importance for the development of controlled chemistry. Recent theoretical advances [177, 178] show that control of the outcome of reactions by use of external fields or coherent superposition of asymptotic states is indeed large.

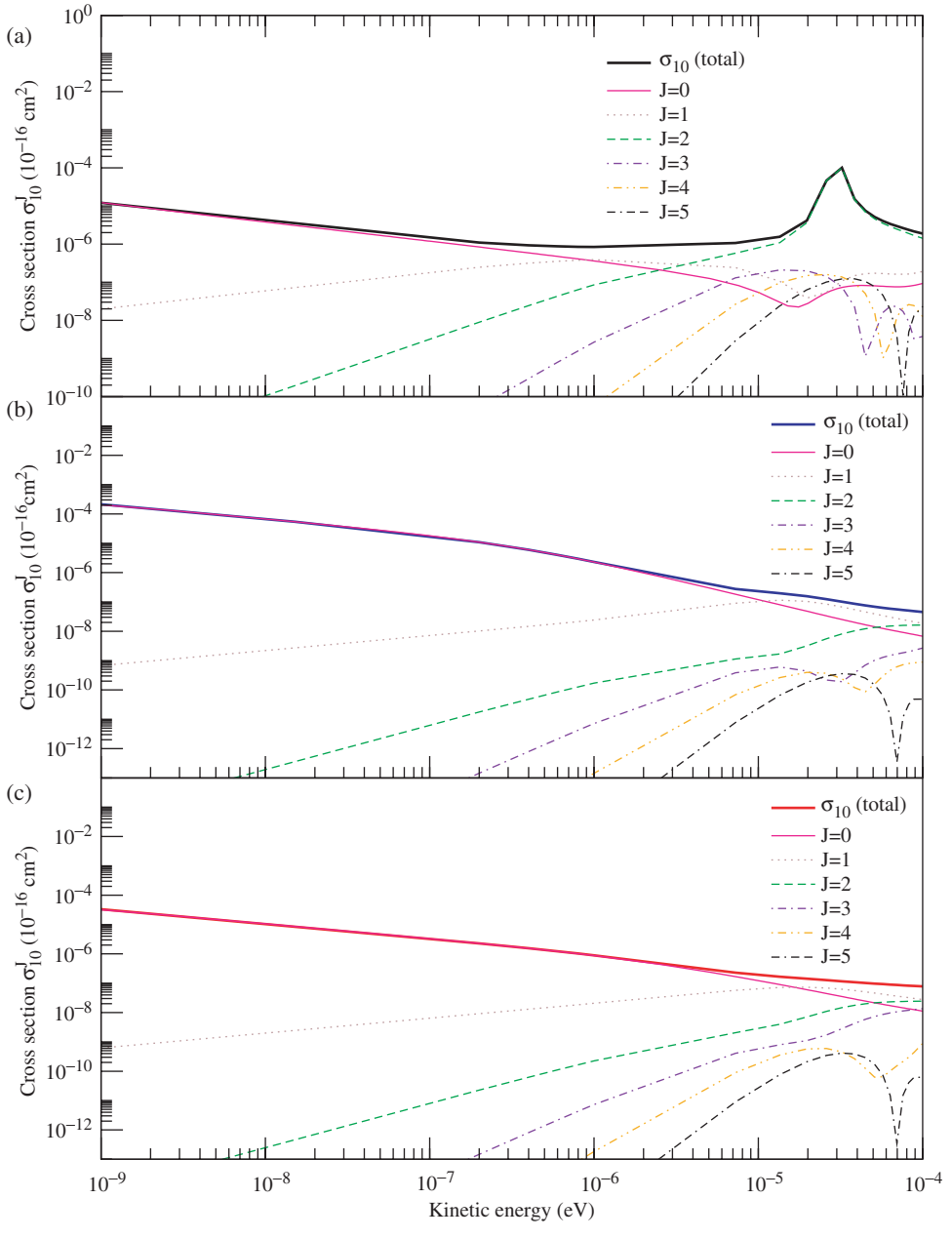

Figure 17. [Colour online] Partial cross-sections for OH formation in $O + H_2(v = 1, j = 0)$ collisions calculated with equation (4) for selected values of the total angular momentum quantum number J. Integral cross-sections from figure 16 have been reproduced for the sake of comparison. (a) GLDP PES [162]; (b) BMS1 PES [176]; (c) BMS2 PES [176].

The rapid development of these research fields should provide support to the current research effort in quantum computers using trapped polar molecules as quantum bits.

In this review we have focused almost exclusively on neutral atom–diatom chemical reactions which occur via tunnelling at low temperatures. As methods to cool and trap different types of molecular systems and clusters become more and more widespread, extensions of these studies to reactive and non-reactive collisions involving ultracold molecules and larger systems will be forthcoming. Also new approaches need to be developed for studying vibrational relaxation and chemical reactivity in highly vibrationally excited ultracold molecules like those created in photoassociation and Feshbach resonance techniques. External control of chemical reactions with electric and magnetic fields is also a topic of active interest, see for example the recent review article by Krems [69]. It is also expected that precise values of atomic and molecular properties derived from cold trapped molecules (such as vibrational/rotational level specific radiative lifetimes and relaxation rate coefficients) may benefit research in atmospheric and astrophysical systems. We refer to the recent work by Meijer and coworkers [32] in this context.

Acknowledgments

This work was supported in part by a grant from the National Science Foundation, Division of Atomic Theory, and the Research Corporation. We thank our collaborators Robert Forrey, Enrico Bodo, Roman Krems, Franco Gianturco, Joao Brandão, and Alex Dalgarno for helpful discussions. We also thank Jeremy Hutson for many useful comments on the manuscript.

References

[1] D. DeMille, Phys. Rev. Lett. **88,** 067901 (2002).
[2] D. DeMille, F. Bay, S. Bickman, D. Kawall, D. Krause, Jr, S. E. Maxwell, and L. R. Hunter, Phys. Rev. A **61,** 052507 (2000).
[3] Y. B. Band and P. S. Julienne, Phys. Rev. A **51,** R4317 (1995).
[4] J. Weiner, V. S. Bagnato, S. Zillo, and P. S. Julienne, Rev. Mod. Phys. **71,** 1 (1999).
[5] J. T. Bahns, P. L. Gould, and W. C. Stwalley, Advan. At. Mol. Opt. Phys. **42,** 171 (2000).
[6] C. J. Williams and P. S. Julienne, Science **287,** 986 (2000).
[7] J. M. Doyle, B. Friedrich, J. Kim, and D. Patterson, Phys. Rev. A **52,** R2515 (1995).
[8] J. M. Doyle and B. Friedrich, Nature **401,** 749 (1999).
[9] J. D. Weinstein, R. deCarvalho, T. Guillet, B. Friedrich, and J. M. Doyle, Nature **395,** 148 (1998).
[10] G. Meijer, Chem. Phys. Chem. **3,** 495 (2002).
[11] K. E. Strecker, G. B. Partridge, and R. G. Hulet, Phys. Rev. Lett. **91,** 080406 (2003).
[12] C. Chin, T. Kraemer, M. Mark, J. Herbig, P. Waldburger, H.-C. Nägerl, and R. Grimm, Phys. Rev. Lett. **94,** 123201 (2005).
[13] D. J. Heinzen, R. Wynar, P. D. Drummond, and K. V. Kheruntsyan, Phys. Rev. Lett. **84,** 5029 (2000).
[14] R. Wynar, R. S. Freeland, D. J. Han, C. Ryu, and D. J. Heinzen, Science **287,** 1016 (2000).
[15] N. Balakrishnan and A. Dalgarno, Chem. Phys. Lett. **341,** 652 (2001).
[16] J. J. Hope and M. K. Olsen, Phys. Rev. Lett. **86,** 3220 (2001).
[17] M. W. Zwierlein, C. A. Stan, C. H. Schunk, S. M. F. Raupach, S. Gupta, Z. Hadzibabic, and W. Ketterle, Phys. Rev. Lett. **91,** 250401 (2003).
[18] M. Greiner, C. A. Regal, and D. S. Jin, Nature **426,** 537 (2003).
[19] S. Jochim, M. Bartenstein, A. Altmeyer, G. Hendl, C. Chin, H. Denschlag, and R. Grimm, Phys. Rev. Lett. **91,** 240402 (2003).

[20] E. A. Donley, N. R. Claussen, S. T. Thompson, and C. E. Wieman, Nature **417,** 529 (2002).
[21] R. deCarvalho, J. M. Doyle, B. Friedrich, T. Guillet, D. Patterson, and J. D. Weinstein, Eur. Phys. J. D **7,** 289 (1999).
[22] B. Friedrich, D. Weinstein, R. deCarvalho, and J. M. Doyle, J. Chem. Phys. **110,** 2376 (1999).
[23] J. A. Maddi, T. P. Dinneen, and H. Gould, Phys. Rev. A **60,** 3882 (1999).
[24] H. L. Bethlem, G. Berden, and G. Meijer, Phys. Rev. Lett. **83,** 1558 (1999).
[25] H. L. Bethlem, G. Berden, A. J. A. van Roij, F. M. H. Crompvoets, and G. Meijer, Phys. Rev. Lett. **84,** 5744 (2000).
[26] H. L. Bethlem, G. Berden, F. M. H. Crompvoets, R. T. Jongma, A. J. A. van Roij, and G. Meijer, Nature **406,** 481 (2000).
[27] H. L. Bethlem, F. M. H. Crompvoets, R. T. Jongma, S. Y. T. van de Meerakker, and G. Meijer, Phys. Rev. A **65,** 053416 (2002).
[28] H. L. Bethlem, A. J. A. van Roij, R. T. Jongma, and G. Meijer, Phys. Rev. Lett. **88,** 13003 (2002).
[29] F. M. H. Crompvoets, H. L. Bethlem, R. T. Jongma, and G. Meijer, Nature **411,** 174 (2001).
[30] S. Y. T. van de Meerakker, R. T. Jongma, and G. Meijer, Phys. Rev. A **64,** 041401(R) (2002).
[31] M. Gupta and D. Herschbach, J. Phys. Chem. A **105,** 1626 (2001).
[32] S. Y. T. van de Meerakker, N. Vanhaecke, M. P. J. van der Loo, G. C. Groenenboom, and G. Meijer, Phys. Rev. Lett. **95,** 013003 (2005).
[33] A. B. Meinel, Astrophys. J. **112,** 120 (1950).
[34] L. S. Rothman *et al*., J. Quant. Spectrosc. Radiat. Transfer, **96,** 139 (2004).
[35] N. Balakrishnan, and A. Dalgarno, J. Phys. Chem. A **107,** 7101 (2003).
[36] P. F. Weck and N. Balakrishnan, Euro. Phys. J. D **31,** 417 (2004).
[37] N. Balakrishnan, J. Chem. Phys. **121,** 5563 (2004).
[38] P. F. Weck and N. Balakrishnan, J. Chem. Phys. **122,** 154309 (2005).
[39] P. F. Weck and N. Balakrishnan, J. Chem. Phys. **122,** 234310 (2005).
[40] P. F. Weck and N. Balakrishnan, J. Chem. Phys. **123,** 144307 (2005).
[41] P. F. Weck, N. Balakrishnan, J. Brandão, C. Rosa, and W. Wang, J. Chem. Phys. **124,** 074308 (2006).
[42] P. F. Weck and N. Balakrishnan, J. Phys. B, in press (2006).
[43] N. Balakrishnan, R. C. Forrey, and A. Dalgarno, Chem. Phys. Lett. **280,** 1 (1997).
[44] N. Balakrishnan, V. Kharchenko, R. C. Forrey, and A. Dalgarno, Chem. Phys. Lett. **280,** 5 (1997).
[45] N. Balakrishnan, R. C. Forrey, and A. Dalgarno, Phys. Rev. Lett. **80,** 3224 (1998).
[46] R. C. Forrey, N. Balakrishnan, V. Kharchenko, and A. Dalgarno, Phys. Rev. A **58,** R2645 (1998).
[47] R. C. Forrey, N. Balakrishnan, A. Dalgarno, M. R. Haggerty, and E. J. Heller, Phys. Rev. Lett. **82,** 2657 (1999).
[48] R. C. Forrey, V. Kharchenko, N. Balakrishnan, and A. Dalgarno, Phys. Rev. A **59,** 2146 (1999).
[49] N. Balakrishnan, R. C. Forrey, and A. Dalgarno, J. Chem. Phys. **113,** 621 (2000).
[50] N. Balakrishnan and A. Dalgarno, J. Phys. Chem. A **105,** 2348 (2001).
[51] C. Zhu, N. Balakrishnan, A. Dalgarno J. Chem. Phys. **115,** 1335 (2001).
[52] R. C. Forrey, N. Balakrishnan, A. Dalgarno, M. R. Haggerty, and E. J. Heller, Phys. Rev. A **64,** 022706 (2001).
[53] P. E. Siska, J. Chem. Phys. **115,** 4527 (2001).
[54] R. C. Forrey, Phys. Rev. A **66,** 023411 (2002).
[55] J. C. Flasher and R. C. Forrey, Phys. Rev. A **65,** 032710 (2002).
[56] E. Bodo, F. A. Gianturco, and A. Dalgarno, Chem. Phys. Lett. **353,** 127 (2002).
[57] N. Balakrishnan, G. C. Groenenboom, R. V. Krems, and A. Dalgarno, J. Chem. Phys. **118,** 7386 (2003).
[58] R. V. Krems, A. Dalgarno, N. Balakrishnan, and G. C. Groenenboom, Phys. Rev. A **67,** 060703(R) (2003).
[59] T. Stoecklin, A. Voronin, and J. C. Rayez, Phys. Rev. A **68,** 032716 (2003).
[60] E. Bodo and F. A. Gianturco, J. Chem. Phys. **107,** 7328 (2003).
[61] K. Tilford, M. Hoster, P. M. Florian, and R. C. Forrey, Phy. Rev. A **69,** 052705 (2004).
[62] P. Florian, M. Hoster, and R. C. Forrey, Phys. Rev. A **70,** 032709 (2004).
[63] T. Stoecklin, A. Voronin, and J. C. Rayez, Chem. Phys. **298,** 175 (2004).
[64] E. Pollak and R. Naaman, Chem Phys. Lett. **123,** 352 (1986).
[65] T. Takayanagi and Y. Kurosaki, J. Chem. Phys. **109,** 8929 (1998).
[66] D. Skouteris, D. E. Manolopoulos, W. S. Bian, H.-J. Werner, L. H. Lai, and K. Liu, Science **286,** 1713 (1999).
[67] T. Takayanagi and A. Wada, Chem. Phys. Lett. **338,** 195 (2001).
[68] T. Xie, D. Wang, J. M. Bowman, and D. E. Manolopoulos, J. Chem. Phys. **116,** 7461 (2002).
[69] R. V. Krems, Int. Rev. Phys. Chem. **24,** 99 (2005).
[70] J. Doyle, B. Friedrich, R. V. Krems, and F. Masnou-Seeuws, Eur. Phys. J. D. **31,** 149 (2004).
[71] D. Skouteris, J. F. Castillo and D. E. Manolopoulos, Comput. Phys. Commun. **133,** 128 (2000).

[72] P. Soldán, M. T. Cvitaš, J. M. Hutson, P. Honvault, and J. M. Launay, Phys. Rev. Lett. **89,** 153201 (2002).
[73] M. T. Cvitaš, P. Soldán, J. M. Hutson, P. Honvault, and J. M. Launay, Phys. Rev. Lett. **94,** 033201 (2005).
[74] M. T. Cvitaš, P. Soldán, J. M. Hutson, P. Honvault, and J. M. Launay, Phys. Rev. Lett. **94,** 200402 (2005).
[75] G. Quéméner, P. Honvault, J. M. Launay, P. Soldán, D. E. Potter, and J. M. Hutson, Phys. Rev. A **71,** 032722 (2005).
[76] E. Bodo and F. A. Gianturco, Phys. Rev. A **73,** 32702 (2006).
[77] E. Bodo, M. Lara, and F. A. Gianturco, J. Chem. Phys. **124,** 44308 (2006).
[78] E. P. Wigner, Phys. Rev. **73,** 1002 (1948).
[79] L. D. Landau and E. Lifshitz, *Quantum Mechanics* (Pergamon Press, Oxford, 1977).
[80] H. R. Sadeghpour, J. L. Bohn, M. J. Cavagnero, B. D. Esry, I. I. Fabrikant, J. H. Macek, and A. R. P. Rau, J. Phys. B: At. Mol. Opt. Phys. **33,** R93 (2000).
[81] T. Takayanagi, N. Masaki, K. Nakamura, M. Okamoto, and G. C. Schatz, J. Chem. Phys. **86,** 6133 (1987).
[82] G. C. Hancock, C. A. Mead, D. G. Truhlar, and A. J. C. Varandas, J. Chem. Phys. **91,** 3492 (1989).
[83] T. Takayanagi, and S. Sato, J. Chem. Phys. **92,** 2862 (1990).
[84] T. Takayanagi, and N. Masaki, J. Chem. Phys. **96,** 4154 (1991).
[85] K. Stark and H.-J. Werner, J. Chem. Phys. **104,** 6515 (1996).
[86] D. E. Manolopoulos, K. Stark, H.-J. Werner, D. W. Arnold, S. E. Bradforth, and D. M. Neumark, Science, **262,** 1852 (1993).
[87] E. Rosenman, S. Hochman-Kowal, A. Persky, and M. Baer, Chem. Phys. Lett. **257,** 421 (1996).
[88] E. Rosenman, A. Persky, and M. Baer, Chem. Phys. Lett. **258,** 639 (1996).
[89] J. F. Castillo, D. E. Manolopoulos, K. Stark, and H.-J. Werner, J. Chem. Phys. **104,** 6531 (1996).
[90] C. L. Russel and D. E. Manolopoulos, Chem. Phys. Lett. **256,** 465 (1996).
[91] T. Takayanagi and Y. Kurosaki, Chem. Phys. Lett. **286,** 35 (1998).
[92] M. H. Alexander, H.-J. Werner, and D. E. Manolopoulos, J. Chem. Phys. **109,** 5710 (1998).
[93] M. Baer, Chem. Phys. Lett. **312,** 203 (1999).
[94] M. Baer, M. Faubel, B. Martínez-Haya, L. Rusin, U. Tappe, and J. P. Toennies, J. Chem. Phys. **110,** 10231 (1999).
[95] F. J. Aoiz, L.Bañares, and J. F. Castillo, J. Chem. Phys. **111,** 4013 (1999).
[96] R. T. Skodge, D. Skouteris, D. E. Manolopoulos, S.-H. Lee, F. Dong, and K. Liu, J. Chem. Phys. **112,** 4536 (2000).
[97] R. T. Skodge, D. Skouteris, D. E. Manolopoulos, S.-H. Lee, F. Dong, and K. Liu, Phys. Rev. Lett. **85,** 1206 (2000).
[98] D. H. Zhang, S.-Y. Lee, and M. Baer, J. Chem. Phys. **112,** 9802 (2000).
[99] S. D. Chao and R. T. Skodge, J. Chem. Phys. **113,** 3487 (2000).
[100] M. H. Alexander, D. E. Manolopoulos, and H.-J. Werner, J. Chem. Phys. **113,** 11084 (2000).
[101] K. Liu, Ann. Rev. Phys. Chem. **52,** 139 (2001).
[102] S.-H. Lee, F. Dong, and K. Liu, J. Chem. Phys. **116,** 7839 (2002).
[103] S. D. Chao and R. T. Skodge, J. Chem. Phys. **119,** 1462 (2003).
[104] V. Aquilanti, S. Cavalli, D. De Fazio, A. Volpi, A. Aguilar, X. Giménez, and J. M. Lucas, Chem. Phys. Lett. **371,** 504 (2003).
[105] V. Aquilanti, S. Cavalli, A. Simoni, A. Aguilar, and J. M. Lucas, J. Chem. Phys. **121,** 11675 (2004).
[106] H. Kornweitz and A. Perky, J. Phys. Chem. **108,** 8599 (2004).
[107] V. Aquilanti, S. Cavalli, D. De Fazio, A. Simoni, and T. V. Tscherbul, J. Chem. Phys. **123,** 054314 (2005).
[108] E. Bodo, F. A. Gianturco, and A. Dalgarno, J. Phys. B: At. Mol. Opt. Phys. **35,** 2391 (2002).
[109] E. Bodo, F. A. Gianturco, and A. Dalgarno, J. Chem. Phys. **116,** 9222 (2002).
[110] E. Bodo and F. A. Gianturco, Eur. Phys. J. D **31,** 423 (2004).
[111] E. Bodo, F. A. Gianturco, N. Balakrishnan, and A. Dalgarno, J. Phys. B: At. Mol. Opt. Phys. **37,** 3641 (2004).
[112] N. Uudus, S. Magaki, and N. Balakrishnan, J. Chem. Phys. **122,** 024304 (2005).
[113] C. Bissonnette, C. E. Chuaqui, K. G. Crowell, and R. J. Le Roy, J. Chem. Phys. **105,** 2639 (1996).
[114] D. W. Schwenke, S. P. Walsh, and P. R. Taylor, J. Chem. Phys. **98,** 4738 (1993).
[115] F. J. Aoiz and L. Bañares, Chem. Phys. Lett. **247,** 232 (1995).
[116] H. Wang, W. H. Thompson, and W. H. Miller, J. Chem. Phys. **107,** 7194 (1997).
[117] U. Manthe, W. Bian, and H.-J. Werner, Chem. Phys. Lett. **313,** 647 (1999).
[118] S. A. Kandel, A. J. Alexander, Z. H. Kim, R. N. Zare, F. J. Aoiz, L. Bañares, J. F. Castillo, and V. S. Rábanos, J. Chem. Phys. **112,** 670 (2000).

[119] W. Bian and H.-J. Werner, J. Chem. Phys. **112,** 220 (2000).
[120] F. Dong, S.-H. Lee, and K. Liu, J. Chem. Phys. **115,** 1197 (2001).
[121] F. J. Aoiz, L. Bañares, J. F. Castillo, M. Menéndez, D. Skouteris, and H.-J. Werner, J. Chem. Phys. **115,** 2074 (2001).
[122] V. Aquilanti, S. Cavalli, F. Pirani, A. Volip, and D. Cappelletti, J. Phys. Chem. A **105,** 2401 (2001).
[123] M. H. Alexander, G. Capecchi, and H. J. Werner, Science **296,** 715 (2002).
[124] M. Balucani, D. Skouteris, L. Cartechini, G. Capozza, E. Segolini, P. Casavecchia, M. H. Alexander, G. Capecchi, and H.-J. Werner, Phys. Rev. Lett. **91,** 013201 (2003).
[125] M.-D. Chen, K.-L. Han, and N.-Q. Lou, J. Chem. Phys. **118,** 4463 (2003).
[126] M. Wang and W. Bian, Chem. Phys. Lett. **391,** 354 (2004).
[127] R. L. Wilson, Z. M. Loh, D. A. Wild, E. J. Bieske, and A. A. Buchachenko, H. J. Chem. Phys. **121,** 2085 (2004).
[128] R. J. Le Roy, G. C. Corey, and J. M. Hutson, Faraday Discuss. Chem. Soc. **73,** 339 (1982).
[129] C. J. Ashton, M. S. Child, and J. M. Hutson, J. Chem. Phys. **78,** 4025 (1982).
[130] D. R. Herschbach, Adv. Chem. Phys. **10,** 319 (1966).
[131] C. H. Becker, P. Casavecchia, P. W. Tiedermann, J. J. Valentini, and Y. T. Lee, J. Chem. Phys. **73,** 2833 (1980).
[132] H. J. Loesch and F. Stienkemeier, J. Chem. Phys. **99,** 9598 (1993).
[133] M. Baer, I. Last, and H.-J. Loesch, J. Chem. Phys. **101,** 9648 (1994).
[134] F. J. Aoiz, M. T. Martinez, M. Menéndez, V. Rábanos, and E. Verdasco, Chem. Phys. Lett. **299,** 25 (1999).
[135] F. J. Aoiz, E. Verdasco, V. S. Rábanos, H.-J. Loesch, M. Menéndez, and F. Stienkemeier, Phys. Chem. Chem. Phys. **2,** 541 (2000).
[136] P. Casavecchia, Rep. Prog. Phys. **63,** 355 (2000).
[137] O. Hobel, M. Menéndez, and H.-J. Loesch, Phys. Chem. Chem. Phys. **3,** 3633 (2001)
[138] F. J. Aoiz, M. T. Martinez, and V. S. Rábanos, J. Chem. Phys. **114,** 8880 (2001).
[139] O. Hobel, R. Bobbenkamp, A. Paladini, A. Russo, and H.-J. Loesch, Phys. Chem. Chem. Phys. **6,** 2198 (2004).
[140] G. A. Parker, A. Laganà, S. Crocchianti, and R. T. Pack, J. Chem. Phys. **102,** 1238 (1995).
[141] F. Gögtas, G. G. Balint-Kurti, and A. R. Offer, J. Chem. Phys. **104,** 7927 (1996).
[142] A. Aguado, M. Paniagua, M. Lara, and O. Roncero, J. Chem. Phys. **106,** 1013 (1997).
[143] A. Aguado, M. Paniagua, M. Lara, and O. Roncero, J. Chem. Phys. **107,** 10085 (1997).
[144] M. Lara, A. Aguado, O. Roncero, and M. Paniagua, J. Chem. Phys. **109,** 9391 (1998).
[145] M. Paniagua, A. Aguado, M. Lara, and O. Roncero, J. Chem. Phys. **109,** 2971 (1998).
[146] M. Lara, A. Aguado, M. Paniagua, and O. Roncero, J. Chem. Phys. **113,** 1781 (2000).
[147] L. Wei, A. W. Jasper, and D. G. Truhlar, J. Phys. Chem. A **107,** 7236 (2003).
[148] A. Laganà, S. Crocchianti and V. Piermarini, Lect. Notes Comp. Science **3044,** 422 (2004).
[149] A. Aguado, M. Paniagua, C. Sanz, and O. Roncero, J. Chem. Phys. **119,** 10088 (2003).
[150] P. S. Zuev, R. S. Sheridan, T. V. Albu, D. G. Truhlar, D. A. Hrovat, and W. T. Borden, Science **299,** 867 (2003).
[151] P. Soldán, M. T. Cvitaš, and J. M. Hutson, Phys. Rev. A **67,** 054702 (2003).
[152] B. R. Johnson and N. W. Winter, J. Chem. Phys. **66,** 4116 (1977).
[153] D. C. Clary, J. N. L. Connor, and C. J. Edge, Chem. Phys. Lett. **68,** 154 (1979).
[154] S. P. Walch, A. F. Wagner, T. H. Dunning Jr, and G. C. Schatz, J. Chem. Phys. **72,** 2894 (1980).
[155] G. C. Schatz, A. F. Wagner, S. P. Walch, and J. M. Bowman, J. Chem. Phys. **74,** 4984 (1981).
[156] J. M. Bowman, A. F. Wagner, S. P. Walch, and T. H. Dunning, J. Chem. Phys. **81,** 1739 (1984).
[157] M. Broida and A. Persky, J. Chem. Phys. **80,** 3687 (1984).
[158] G. C. Schatz, J. Chem. Phys. **83,** 5667 (1985).
[159] B. C. Garrett, D. G. Truhlar, and G. C. Schatz, J. Am. Chem. Soc. **108,** 2867 (1986).
[160] T. Joseph, D. G. Truhlar, and B. C. Garret, J. Chem. Phys. **88,** 6982 (1988).
[161] D. C. Chatfield, R. S. Friedman, G. C. Lynch, D. G. Truhlar, and D. W. Schwenke, J. Chem. Phys. **98,** 342 (1993).
[162] S. Rogers, D. Wang, A. Kuppermann, and S. Walch, J. Phys. Chem. A **104,** 2308 (2000).
[163] M. R. Hoffmann and G. C. Schatz, J. Chem. Phys. **113,** 9456 (2000).
[164] D. J. Garton, T. K. Minton, B. Maiti, D. Troya, and G. C. Schatz, J. Chem. Phys. **118,** 1585 (2003).
[165] N. Balakrishnan, J. Chem. Phys. **119,** 195 (2003).
[166] B. Maiti and G. C. Schatz, J. Chem. Phys. **119,** 12360 (2003).
[167] M. Braunstein, S. Adler-Golden, B. Maiti, and G. C. Schatz, J. Chem. Phys. **120,** 4316 (2004).
[168] N. Balakrishnan, J. Chem. Phys. **121,** 6346 (2004).
[169] A. A. Westenberg and N. deHaas, J. Chem. Phys. **47,** 4721 (1967).
[170] A. A. Westenberg and N. deHaas, J. Chem. Phys. **50,** 2512 (1969).

[171] G. C. Light, J. Chem. Phys. **68,** 2831 (1978).
[172] N. Cohen and K. Westburg, J. Phys. Chem. Ref. Data, **12,** 531 (1983).
[173] N. Presser and R. J. Gordon, J. Chem. Phys. **82,** 1291 (1985).
[174] D. C. Robie, S. Arepalli, N. Presser, T. Kitsopoulos, and R. J. Gordon, Chem. Phys. Lett. **134,** 579 (1987).
[175] D. L. Baulch, C. J. Cobos, R. A. Cox, C. Esser, P. Frank, Th. Just, J. A. Kerr, M. J. Pilling, J. Troe, R. W. Walker, and J. Warnatz, J. Phys. Chem. Ref. Data **21,** 411 (1992).
[176] J. Brandão, C. Mogo, and B. C. Silva, J. Chem. Phys. **121,** 8861 (2004).
[177] V. Zeman, M. Shapiro, and P. Brumer, Phys. Rev. Lett. **92,** 133204 (2004).
[178] R. Krems, Phys. Rev. Lett. **96,** 123202 (2006).